Chemical Science

EDGE ARTICLE

View Article Online
View Journal | View Issue

Cite this: *Chem. Sci.*, 2014, **5**, 3130

A dual-fluorescent composite of graphene oxide and poly(3-hexylthiophene) enables the ratiometric detection of amines†

Dongli Meng,[a] Shaojun Yang,[a] Dianming Sun,[b] Yi Zeng,[a] Jinhua Sun,[a] Yi Li,[a] Shouke Yan,[b] Yong Huang,[a] Christopher W. Bielawski[cd] and Jianxin Geng*[a]

Received 25th February 2014
Accepted 14th April 2014

DOI: 10.1039/c4sc00598h

www.rsc.org/chemicalscience

A composite prepared by grafting a conjugated polymer, poly(3-hexylthiophene) (P3HT), to the surface of graphene oxide was shown to result in a dual-fluorescent material with tunable photoluminescent properties. Capitalizing on these unique features, a new class of graphene-based sensors that enables the ratiometric fluorescence detection of amine-based pollutants was developed. Moreover, through a detailed spectroscopic study, the origin of the optical properties of the aforementioned composite was studied and was found to be due to electronic decoupling of the conjugated polymer from the GO. The methodology described herein effectively overcomes a long-standing challenge that has prevented graphene based composites from finding utility in sensing and related applications.

Introduction

Fluorescent graphene based materials, particularly those based on graphene oxide (GO), have recently attracted considerable attention on account of their high chemical stability, biocompatibility, and excitation induced nonlinear optical properties.[1] The origin of the aforementioned fluorescence phenomena has been attributed to the relatively large band gap associated with isolated domains of sp^2 hybridized carbons dispersed in a sp^3 hybridized carbon–oxygen matrix[2] as well as the coupling of localized electronic states found in defects.[3] Regardless, many of the fluorescence properties of GO, including its emission wavelength, are closely related to the material's surface chemistry which can be conveniently tuned through chemical modification.[2b,c,4] Similarly, photoluminescence (PL) properties may be realized through the passivation of residual epoxy, carboxyl, and other functional groups that facilitate non-radiative recombination of localized electron–hole pairs.[2b,5] Thus far, saturated and other non-functional polymers, such as various polyolefins and poly(ethylene glycol), have been used to passivate GO,[1a,2b,3b,6] primarily to limit any potentially undesirable photoinduced electron transfer processes.[7]

Herein, we show that a composite prepared by grafting a conjugated polymer, poly(3-hexylthiophene) (P3HT), to the surface of GO results in a material with enhanced PL properties, including tunable photoemission and dual-fluorescence characteristics (Scheme 1a). Capitalizing on this unique combination of features, the aforementioned material was used as a fluorescence sensor to detect amines in a ratiometric fashion. We will also demonstrate that the methodology described below effectively overcomes a long-standing challenge that has curtailed the use of graphene based composites in sensing and related applications.

[a]National Engineering Research Center of Engineering Plastics, Technical institute of Physics and Chemistry, Chinese Academy of Sciences, 29 Zhongguancun East Road, Haidian District, Beijing 100190, China. E-mail: jianxingeng@mail.ipc.ac.cn; Fax: +86-6255 4670; Tel: +86-8254 3416

[b]State Key Laboratory of Chemical Resource Engineering, Beijing University of Chemical Technology, 15 Beisanhuan East Road, Chaoyang District, Beijing 100029, China

[c]Department of Chemistry, University of Texas at Austin, 1 University Station, A1590, Austin, Texas 78712, USA

[d]Department of Chemistry, Ulsan National Institute of Science and Technology, 50 UNIST-gil, Ulju-gun, Ulsan 689-798, South Korea

† Electronic supplementary information (ESI) available: Synthesis and characterization of GO/P3HT and GO/HA composites, theoretical calculations, TEM images of the GO/HA composite, confocal fluorescence images of the GO/P3HT composite, fluorescence responses of GO and the GO/HA composite to aniline and nitrobenzene. See DOI: 10.1039/c4sc00598h

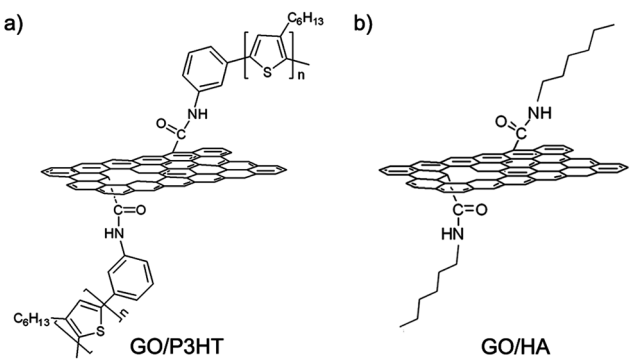

Scheme 1 Structures of the GO/P3HT and GO/HA composites.

Results and discussion

The GO composite was synthesized by condensing the residual carboxylic acid groups present on the GO surface with amino-terminated P3HT. The composite was designated as GO/P3HT. As a control, a non-functional analogue, GO/HA, was prepared by condensing 1-hexylamine with GO (Scheme S1†). Details of the reactions are included in the ESI.† The grafting densities of the aforementioned materials were controlled by adjusting the initial amine : GO ratio, as determined by thermogravimetric analysis (Fig. S1†). The GO/P3HT and GO/HA composites showed improved dispersibilities in common organic solvents, including chloroform, tetrahydrofuran, and chlorobenzene.[8]

With GO/P3HT and GO/HA in hand, the UV-visible and PL spectra of the composites were recorded in order to ascertain the effect of the grafts on the optical properties of the resulting materials (Fig. 1). While a suspension of GO in water exhibited an absorbance at 234 nm and a shoulder peak at *ca.* 300 nm, due to the π–π* and n–π* transitions of the C=C and C=O bonds, respectively, the signals of the π–π* transition measured for the suspensions of the GO/P3HT or GO/HA composites in chloroform were bathochromically shifted to *ca.* 270 nm. Additionally, the GO/P3HT composite displayed three additional absorbance maxima at 457, 586, and 642 nm, which were attributed to the P3HT component (Fig. 1a), although these signals appeared to be split which may reflect a stacked, polymeric structure[9] due to the GO induced assembly[10] or grafting induced aggregation.[11],‡ As summarized in Fig. 1b, the GO/HA composite showed a single PL emission that peaked at 523 nm upon excitation at 460 nm; such fluorescence properties were similar to those observed in other materials derived from GO.[6] In contrast, upon excitation at 340 nm, the GO/P3HT composite exhibited well-resolved PL signals centred at 421 and 578 nm. The former was attributed to the fluorescent centres contained within the GO scaffold, whereas the latter was assigned to the P3HT component. As shown in the inset of Fig. 1b, the suspensions of the GO/HA and GO/P3HT composites appeared green and red-purple, respectively, upon excitation with light at the corresponding wavelength. The blue-shifted PL emission of the GO component in the GO/P3HT composite was attributed to the passivation of the GO surface *via* the charge transfer from P3HT[12] and/or distortion of the sp^2 domains due to chemical modification. In control experiments, the unmodified GO did not show PL emission. This was not in agreement with some references,[13] probably due to the oxidation process used to synthesize the GO. A mixture of GO and P3HT was also physically prepared. The PL emission of P3HT was quenched by GO (Fig. S3†) but the PL features ascribed to the GO component in the GO/P3HT composite were not observed, due to the inexistence of the assembly structures of P3HT in the mixture of GO and P3HT.

Next, efforts were directed toward gaining a deeper understanding of the dual-fluorescence properties displayed by the aforementioned GO/P3HT composite. The PL quantum yield of the GO component in the GO/P3HT composite was measured to be 3.8% when compared to a rhodamine 6G reference; in contrast, the quantum yield of the GO/HA composite was measured to be 1.8% under similar conditions. The enhanced PL emission observed in the former was ascribed to photo-induced electron transfer from P3HT to GO,[14] which was also confirmed by a PL lifetime measurement. As shown in Fig. 2, the lifetime of the PL emission at 421 nm for the GO/P3HT composite was measured to be 1.8 ns whereas the lifetime of the emission from the GO/HA composite was 1.5 ns; both of these values were in agreement with literature reports.[2c] Collectively, these data revealed that the PL emission at 421 nm was due to the fluorescent centres contained within the GO scaffold. Moreover, the PL emission at 578 nm for the GO/P3HT composite was found to display a PL lifetime of 180 ps, which is shorter than that for pure P3HT (460 ps), a result that reflected the photo-induced electron transfer from P3HT to GO in the GO/P3HT composite.

Although covalent interactions between the P3HT chains and the GO scaffold were reported to quench fluorescence,[7a,15] the P3HT appeared to be decoupled from potential intra- or intermolecular exciton migration pathways as evidenced by the

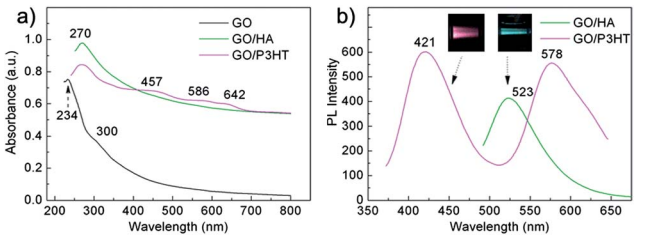

Fig. 1 (a) UV-visible absorption spectra of a GO suspension in deionized water (0.03 mg mL^{-1}), and suspensions of the GO/P3HT and GO/HA composites in chloroform (0.03 mg mL^{-1}). (b) PL spectra of suspensions of the GO/P3HT composite (λ_{ex} = 340 nm) and the GO/HA composite (λ_{ex} = 460 nm). Inset: images of the fluorescence of the GO/P3HT and GO/HA composite suspensions excited with corresponding wavelengths.

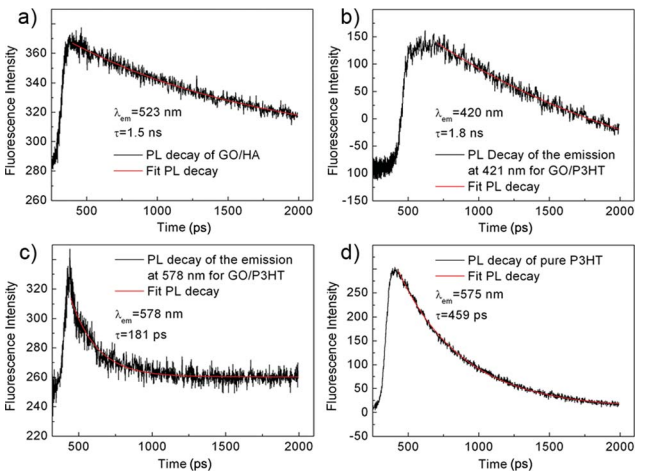

Fig. 2 PL decay curves of (a) the GO/HA composite, (b) the PL emission at 421 nm for the GO/P3HT composite, (c) the PL emission at 578 nm for the GO/P3HT composite, (d) pure P3HT.

two sets of absorption signals observed in the UV-visible absorption spectrum (Fig. 1a).[16] Indeed, the optical properties of the P3HT segments appeared to function independently to those displayed by the GO.

Since excitation dependent and independent PL emissions have been reported for other GO derived materials,[2b,3b,17] subsequent efforts were directed toward comparing the PL properties of the aforementioned composites after excitation at various wavelengths. As shown in Fig. 3a and b, the maximum of the GO-derived photoemission did not significantly change after excitation at wavelengths ranging from 300 to 370 nm for the GO/P3HT composite and from 300 to 480 nm for the GO/HA composite. The consistent energy of the PL emission may be due to the relatively uniform size of the sp^2 domains present in the GO component, which may cause the nano-sized sp^2 domains to function in a manner consistent with a small molecule chromophore. Conversely, the intensity of the PL emission of the GO component was found to vary as a function of the excitation wavelength, with the strongest PL emission recorded after excitation at 340 nm (Fig. 3c). Moreover, the relationship between the intensity of the PL emission and the excitation wavelength was in agreement with the PL excitation (PLE) spectrum recorded at 421 nm. The single peak recorded in the PLE spectrum of the GO/P3HT composite may be related to various electronic structures present on the surface of the material. For comparison, the PLE spectrum of the GO/HA composite, recorded after excitation at 523 nm, displayed three signals at 309, 359, and 465 nm (Fig. 3d), which were attributed to three unique electron transition processes.

As summarized in Fig. 4, the aforementioned assignments were supported by theoretical calculations.[18] Fig. 4a displays three structural models of the GO/HA composites, wherein the hexyl groups were connected to the GO basal plane at different positions. In these models, the C : O ratio and the number of

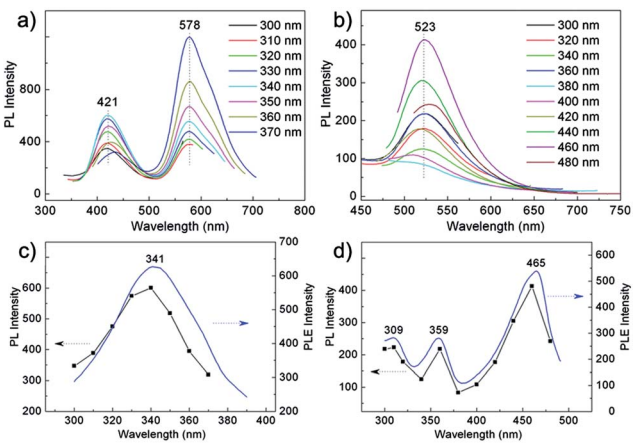

Fig. 3 PL spectra of suspensions of (a) the GO/P3HT composite and (b) the GO/HA composite excited with various wavelengths (indicated). (c) PLE spectrum of the GO/P3HT composite (solid line) and the intensity of the PL emission at 421 nm as a function of the excitation wavelength (squares). (d) PLE spectrum of the GO/HA composite (solid line) and the intensity of the PL emission at 523 nm as a function of the excitation wavelength (squares).

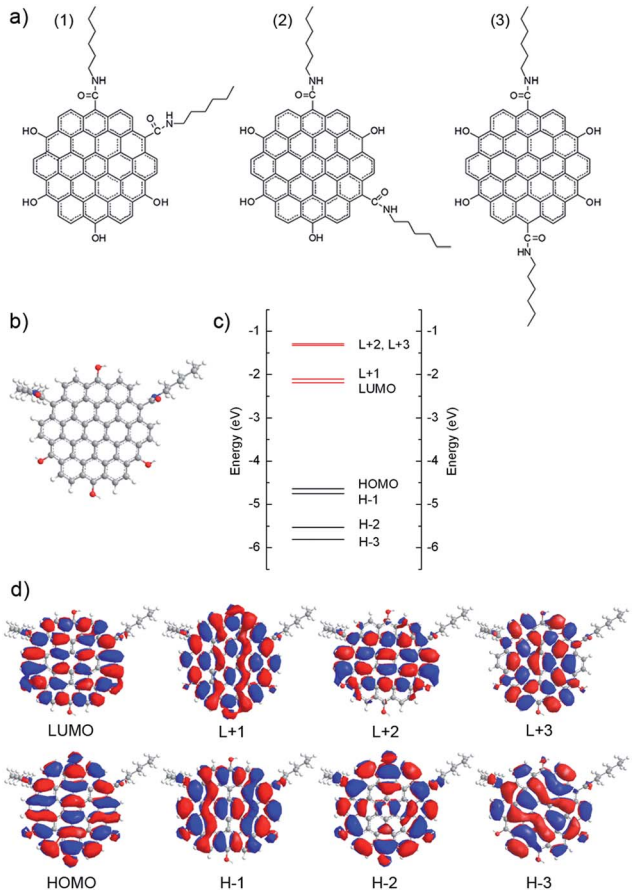

Fig. 4 Band structure calculations of the GO/HA composite: (a) three different structural models, (b) ball-and-spoke representation of (2), (c) molecular orbital energy diagram of (2), (d) molecular orbitals of (2).

substituent hexyl groups were determined based on XPS data. Because the electronic orbitals were localized on the conjugated graphene sheets, the orbital energy levels calculated for these structures were found to be similar; as such, the results of structure (2), which is shown in Fig. 4b, are discussed below. As summarized in Fig. 4c, the energy differences between HOMO/H−1 and LUMO/L+1 range from 2.45 to 2.66 eV, and may be assigned to the peak at 465 nm recorded in the PLE spectrum (Fig. 3d). Likewise, the energy differences between HOMO/H−1 and L+2/L+3, as well as H−2/H−3 and LUMO/L+1, range from 3.31 to 3.47 eV, and may be attributed to the peak recorded at 359 nm. Finally, the signal at 309 nm can be assigned to the energy differences between H−2/H−3 and L+2/L+3, which range from 4.20 to 4.51 eV. Thus, upon excitation, the electrons appear to relax to a low-lying LUMO and then to a lower energy level concomitant with PL emission.

In parallel, the molecular orbital energy levels of a GO/P3HT composite were also calculated and compared to the results described above. In order to simply the calculations, sexithiophene was used *in lieu* of a high molecular weight P3HT chain. As summarized in Fig. S4,† the differences between the molecular orbital energy levels such as the HOMO, H−1, H−2, and H−3, as well as the LUMO, L+1, L+2, and L+3 are not

separated as greatly as those calculated for the GO/HA composite. As such, the conjugated substituent is electronically coupled to the graphene sheets and explains the single peak recorded in the PLE spectrum of the GO/P3HT composite.

The morphologies of the aforementioned GO/P3HT composite were also studied using transmission electron microscopy (TEM). As summarized in Fig. 5, the GO/P3HT composite exhibited a broad distribution of sizes that included sheets of *ca.* 100 nm in size and particles of *ca.* 10 nm in diameter. The small sized particles may have been formed during the amidation reaction since no such sized particles were observed in unmodified samples of GO. In addition, the GO/P3HT composite showed rough surfaces and high-contrast edges, which may be due to the higher grafting density near the holes in the surfaces and at the edges of the GO sheets.[19] Similar morphologies and size distributions were also observed upon TEM analysis of the GO/HA composite (Fig. S5†). Further analysis of the GO/P3HT composite using confocal microscopy (Fig. S6†) revealed that both the large-sized sheets and the small-sized particles were fluorescent, and that the signals derived from the large-sized sheets were of relatively higher intensity.

Finally, we explored the application of our dual-fluorescent GO/P3HT composite as a ratiometric probe for aniline and nitrobenzene. Materials which display ratiometric fluorescence responses based on the intensity ratio of two different PL emissions are often advantageous for use in sensors because the detection process is quantitative and independent of the probe concentration.[20] While aniline and nitrobenzene are valued feedstocks and widely used in the chemical industry, they display carcinogenic and mutagenic properties; thus, rapid and quantitative methods for their detection remains an important analytical target. Currently, the detection of aniline and nitrobenzene is commonly performed by using labour and cost intensive spectrophotometric and chromatographic based techniques.

As shown in Fig. 6a, the intensity of the PL emission of the GO component in the GO/P3HT composite decreased upon exposure to increasing concentrations of aniline,[21] whereas the intensity of the PL emission of the P3HT component remained relatively constant. Moreover, as shown in Fig. 6b, the ratio of the PL intensity of the P3HT component to the PL intensity of the GO component (I_P/I_G) was found to be linearly correlated with the concentration of aniline. Different results were obtained when nitrobenzene was used as the analyte.[21] As shown in Fig. 6c, the PL emission of GO as well as the P3HT components were quenched upon exposure to nitrobenzene and, although linear, the relationship between I_P/I_G and concentration of nitrobenzene changed at high concentrations (Fig. 6d).

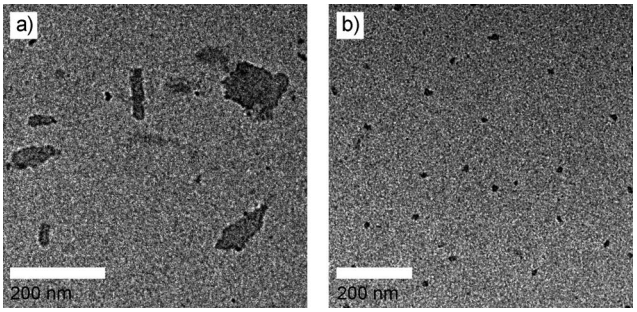

Fig. 5 TEM images of the GO/P3HT composite: (a) large-sized sheets, and (b) small-sized particles.

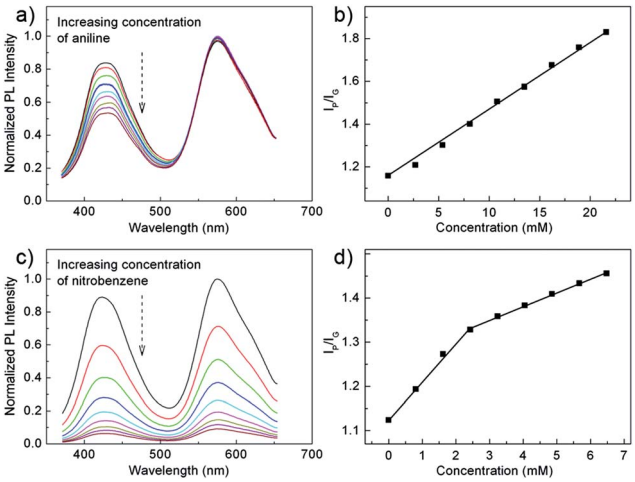

Fig. 6 Normalized PL spectra of the GO/P3HT composite (λ_{ex} = 340 nm) in the presence of various concentrations of (a) aniline and (c) nitrobenzene. Intensity ratio I_P/I_G plotted as function of the concentration of (b) aniline and (d) nitrobenzene.

To explore the aforementioned PL responses in more detail, a series of control experiments were performed. Aniline was found to effectively quench the PL emission of the GO/HA composite but not that of P3HT (Fig. S7†), which indicated that aniline may be selectively interacting with GO. Thus, the GO component served as the active centre to detect aniline in the GO/P3HT composite whereas the P3HT component functioned as an internal PL emission standard. In contrast, nitrobenzene quenched the PL emission of the GO/HA composite as well as pure P3HT (Fig. S8†). This result suggested to us that there were two types of active centres in the GO/P3HT composite for detecting nitrobenzene. As such, the inflection point in the plot of I_P/I_G as function of the concentration of nitrobenzene may reflect the relative sensitivities of these two centres (Fig. S8b†).[22] Regardless, grafting longer chains of P3HT to the GO enhanced the sensitivity of the material and enabled a rapid, quantitative detection of aniline as well as nitrobenzene. Finally, since the solid film of the GO/P3HT composite also displayed dual-fluorescence features, as revealed *via* confocal microscopy (Fig. S6†), the solid films could be used for vapour detection of amine-based pollutants.

Conclusions

In summary, a dual-fluorescent GO/P3HT composite was synthesized by grafting P3HT chains to the surfaces of GO. The GO/P3HT composite showed well-resolved PL emissions at 421

and 578 nm, which were attributed to the GO and P3HT components, respectively. Moreover, the intensity of the emissions were successfully tuned by varying the excitation wavelength. Capitalizing on these properties, we demonstrated, for the first time, that GO based materials may be used to detect organic substrates in a ratiometric manner. Considering the broad number of methods available to modify the structures and properties of GO, we expect that the methodology described herein will be adapted and used to realize new sensors and bestow other carbon materials with useful fluorescence properties and functions.

Acknowledgements

This work was supported by the "Hundred Talents Program" of Chinese Academy of Sciences, the National Natural Science Foundation of China (21274158, 91333114), and the Chinese Academy of Sciences Visiting Professorships for Senior International Scientists (2013T1G0019). CWB is grateful to the BK21 Plus Program, which is funded by the Ministry of Education and the National Research Foundation of Korea.

Notes and references

‡ This hypothesis was corroborated upon spectroscopic analysis of the GO/P3HT composite with the highest grafting density which showed clear splitting of the new absorption bands (Fig. S2†).

1 (*a*) X. Sun, Z. Liu, K. Welsher, J. T. Robinson, A. Goodwin, S. Zaric and H. Dai, *Nano Res.*, 2008, **1**, 203; (*b*) L. Cao, M. J. Meziani, S. Sahu and Y.-P. Sun, *Acc. Chem. Res.*, 2013, **46**, 171; (*c*) H. Sun, L. Wu, N. Gao, J. Ren and X. Qu, *ACS Appl. Mater. Interfaces*, 2013, **5**, 1174; (*d*) B. Senyuk, N. Behabtu, B. G. Pacheco, T. Lee, G. Ceriotti, J. M. Tour, M. Pasquali and I. I. Smalyukh, *ACS Nano*, 2012, **6**, 8060.

2 (*a*) G. Eda, Y.-Y. Lin, C. Mattevi, H. Yamaguchi, H.-A. Chen, I. S. Chen, C.-W. Chen and M. Chhowalla, *Adv. Mater.*, 2010, **22**, 505; (*b*) S. Zhu, J. Zhang, S. Tang, C. Qiao, L. Wang, H. Wang, X. Liu, B. Li, Y. Li, W. Yu, X. Wang, H. Sun and B. Yang, *Adv. Funct. Mater.*, 2012, **22**, 4732; (*c*) C.-T. Chien, S.-S. Li, W.-J. Lai, Y.-C. Yeh, H.-A. Chen, I. S. Chen, L.-C. Chen, K.-H. Chen, T. Nemoto, S. Isoda, M. Chen, T. Fujita, G. Eda, H. Yamaguchi, M. Chhowalla and C.-W. Chen, *Angew. Chem., Int. Ed.*, 2012, **51**, 6662.

3 (*a*) C. Galande, A. D. Mohite, A. V. Naumov, W. Gao, L. J. Ci, A. Ajayan, H. Gao, A. Srivastava, R. B. Weisman and P. M. Ajayan, *Sci. Rep.*, 2011, **1**, 85; (*b*) J. Shen, Y. Zhu, C. Chen, X. Yang and C. Li, *Chem. Commun.*, 2011, **47**, 2580; (*c*) T. Gokus, R. R. Nair, A. Bonetti, M. Bohmler, A. Lombardo, K. S. Novoselov, A. K. Geim, A. C. Ferrari and A. Hartschuh, *ACS Nano*, 2009, **3**, 3963.

4 S. Zhu, J. Zhang, X. Liu, B. Li, X. Wang, S. Tang, Q. Meng, Y. Li, C. Shi, R. Hu and B. Yang, *RSC Adv.*, 2012, **2**, 2717.

5 A. Kundu, R. K. Layek, A. Kuila and A. K. Nandi, *ACS Appl. Mater. Interfaces*, 2012, **4**, 5576.

6 Q. S. Mei, K. Zhang, G. J. Guan, B. H. Liu, S. H. Wang and Z. P. Zhang, *Chem. Commun.*, 2010, **46**, 7319.

7 (*a*) D. S. Yu, Y. Yang, M. Durstock, J. B. Baek and L. M. Dai, *ACS Nano*, 2010, **4**, 5633; (*b*) J. Geng and H. Jung, *J. Phys. Chem. C*, 2010, **114**, 8227; (*c*) J. Sun, D. Meng, S. Jiang, G. Wu, S. Yan, J. Geng and Y. Huang, *J. Mater. Chem.*, 2012, **22**, 18879; (*d*) J. Sun, L. Xiao, D. Meng, J. Geng and Y. Huang, *Chem. Commun.*, 2013, **49**, 5538.

8 (*a*) D. Meng, J. Sun, S. Jiang, Y. Zeng, Y. Li, S. Yan, J. Geng and Y. Huang, *J. Mater. Chem.*, 2012, **22**, 21583; (*b*) S. Niyogi, E. Bekyarova, M. E. Itkis, J. L. McWilliams, M. A. Hamon and R. C. Haddon, *J. Am. Chem. Soc.*, 2006, **128**, 7720.

9 T. Yamamoto, D. Komarudin, M. Arai, B. L. Lee, H. Suganuma, N. Asakawa, Y. Inoue, K. Kubota, S. Sasaki, T. Fukuda and H. Matsuda, *J. Am. Chem. Soc.*, 1998, **120**, 2047.

10 A. Chunder, J. H. Liu and L. Zhai, *Macromol. Rapid Commun.*, 2010, **31**, 380.

11 V. Senkovskyy, R. Tkachov, T. Beryozkina, H. Komber, U. Oertel, M. Horecha, V. Bocharova, M. Stamm, S. A. Gevorgyan, F. C. Krebs and A. Kiriy, *J. Am. Chem. Soc.*, 2009, **131**, 16445.

12 J. Xu, J. Wang, M. Mitchell, P. Mukherjee, M. Jeffries-El, J. W. Petrich and Z. Lin, *J. Am. Chem. Soc.*, 2007, **129**, 12828.

13 X.-F. Zhang, X. Shao and S. Liu, *J. Phys. Chem. A*, 2012, **116**, 7308.

14 Z. X. Gan, S. J. Xiong, X. L. Wu, C. Y. He, J. C. Shen and P. K. Chu, *Nano Lett.*, 2011, **11**, 3951.

15 Y. Liu, J. Zhou, X. Zhang, Z. Liu, X. Wan, J. Tian, T. Wang and Y. Chen, *Carbon*, 2009, **47**, 3113.

16 (*a*) E. Hennebicq, G. Pourtois, G. D. Scholes, L. M. Herz, D. M. Russell, C. Silva, S. Setayesh, A. C. Grimsdale, K. Mullen, J. L. Bredas and D. Beljonne, *J. Am. Chem. Soc.*, 2005, **127**, 4744; (*b*) K. Susumu, P. R. Frail, P. J. Angiolillo and M. J. Therien, *J. Am. Chem. Soc.*, 2006, **128**, 8380.

17 S. Zhuo, M. Shao and S.-T. Lee, *ACS Nano*, 2012, **6**, 1059.

18 S. H. Jin, D. H. Kim, G. H. Jun, S. H. Hong and S. Jeon, *ACS Nano*, 2013, **7**, 1239.

19 (*a*) D. R. Dreyer, S. Park, C. W. Bielawski and R. S. Ruoff, *Chem. Soc. Rev.*, 2010, **39**, 228; (*b*) D. R. Dreyer, A. D. Todd and C. W. Bielawski, *Chem. Soc. Rev.*, 2014, DOI: 10.1039/C4CS00060A.

20 T. Ueno and T. Nagano, *Nat. Methods*, 2011, **8**, 642.

21 B. Das, R. Voggu, C. S. Rout and C. N. R. Rao, *Chem. Commun.*, 2008, 5155.

22 M. de Miguel, M. Alvaro and H. Garcia, *Langmuir*, 2012, **28**, 2849.

